

## An Apamin- and Scyllatoxin-Insensitive Isoform of the Human SK3 Channel

Oliver H. Wittekindt, Violeta Visan, Hiroaki Tomita, Faiqa Imtiaz, Jay J. Gargus, Frank Lehmann-Horn, Stephan Grissmer, and Deborah J. Morris-Rosendahl

*Department of Applied Physiology, University of Ulm, Ulm, Germany (O.H.W., V.V., F.L.-H., S.G.); Institute for Human Genetics and Anthropology, Albert-Ludwigs-University, Freiburg, Germany (O.H.W., D.J.M.-R.); Division of Human Genetics and Department of Pediatrics (J.J.G.), Department of Physiology and Biophysics (H.T., F.I., J.J.G.); and Department of Psychiatry and Human Behavior (H.T.), University of California at Irvine, Irvine, California; and King Faisal Medical Center, Riyadh, Saudi Arabia (F.I.)*

Received July 16, 2003; accepted November 24, 2003

This article is available online at <http://molpharm.aspetjournals.org>

### ABSTRACT

We have isolated an hSK3 isoform from a human embryonic cDNA library that we have named hSK3\_ex4. This isoform contains a 15 amino acid insertion within the S5 to P-loop segment. Transcripts encoding hSK3\_ex4 are coexpressed at lower levels with hSK3 in neuronal as well as in non-neuronal tissues. To investigate the pharmacokinetic properties of hSK3\_ex4, we expressed the isoforms hSK3 and hSK3\_ex4 in tsA cells. Both isoforms were similarly activated by cytosolic  $\text{Ca}^{2+}$  (hSK3,  $\text{EC}_{50} = 0.91 \pm 0.4 \mu\text{M}$ ; hSK3\_ex4,  $\text{EC}_{50} = 0.78 \pm 0.2 \mu\text{M}$ ) and by 1-ethyl-2-benzimidazolinone (hSK3,  $\text{EC}_{50} = 0.17 \text{ mM}$ ; hSK3\_ex4,  $0.19 \text{ mM}$ ). They were both blocked by tetraethylammonium (hSK3,  $K_d = 2.2 \text{ mM}$ ; hSK3\_ex4,  $2.6 \text{ mM}$ ) and showed similar permeabilities relative to  $\text{K}^+$  for  $\text{Cs}^+$  (hSK3,

$0.17 \pm 0.04, n = 3$ ; hSK3\_ex4,  $0.17 \pm 0.05, n = 3$ ) and  $\text{Rb}^+$  (hSK3,  $0.79 \pm 0.04, n = 3$ ; hSK3\_ex4,  $0.8 \pm 0.07, n = 3$ ).  $\text{Ba}^{2+}$  blocked both isoforms, and in both cases, the block was strongest at hyperpolarizing membrane potentials. However, the voltage-dependence of hSK3 was stronger than that of hSK3\_ex4. The most obvious distinguishing feature of this new isoform was that whereas hSK3 was blocked by apamin ( $K_d = 0.8 \text{ nM}$ ), scyllatoxin ( $K_d = 2.1 \text{ nM}$ ), and *d*-tubocurarine ( $K_d = 33.4 \mu\text{M}$ ), hSK3\_ex4 was not affected by apamin up to  $100 \text{ nM}$ , scyllatoxin up to  $500 \text{ nM}$ , and *d*-tubocurarine up to  $500 \mu\text{M}$ . So far, isoform hSK3\_ex4 forms the only small-conductance calcium-activated potassium (SK) channels, which are insensitive to the classic SK blockers.

Small conductance calcium-activated potassium channels (SK channels) form a distinct subfamily of potassium channels, which consists of three members, SK1 to SK3 (Köhler et al., 1996). All have a topology that is typical for potassium channels with six transmembrane helices and a P-loop region. They are voltage-independent and can be activated by elevated cytosolic  $\text{Ca}^{2+}$  concentrations. The activation of all members of this subfamily is mediated by calmodulin, which constitutively binds to the C-terminal cytosolic region of SK channels (Xia et al., 1998; Fanger et al., 1999; Schumacher et

al., 2001). Members of this subfamily are traditionally distinguished by their different sensitivities to apamin (Köhler et al., 1996; Ishii et al., 1997; Grunnet et al., 2001a).

Transcripts of SK1, SK2, and SK3 have been detected in brain tissues, with SK1 expression apparently restricted to brain, whereas SK2 and SK3 are also expressed in non-neuronal tissues (Rimini et al., 2000). SK channels mediate the after-hyperpolarization (AHP) in excitable cells (Köhler et al., 1996; Stocker et al., 1999). These channels modulate the spike frequency of excitable cells, and therefore they are known to play a crucial role in modulating the firing pattern of these cells. The blockage of currents underlying the AHP leads to a burst of action potentials and an increased dopamine release (Stocker et al., 1999; Pedarzani et al., 2001; Savic et al., 2001). In the rat, it has been shown that SK3 channels function as pacemakers in dopaminergic neurons (Wolfart et al., 2001), which outlines SK3 to play a key role in

This work was partially supported by grants from the Deutsche Forschungsgemeinschaft (Gr848/8-2), the Bundesministeriums für Bildung und Forschung (iZKF Ulm, B7), the Faculty of Medicine at the University of Ulm (Project P770), and National Institutes of Health grant MH59222 (to J.J.G.).

This work was presented previously in poster form: Wittekindt OH, Visan V, Tomita H, Imtiaz F, Gargus JJ, Lehmann-Horn F, Grissmer S, and Morris-Rosendahl DJ (2003) A scyllatoxin-insensitive isoform of the human SK3 channel 443-Pos. *Biophys J* 84–2:92a.

**ABBREVIATIONS:** SK channels, small-conductance calcium-activated potassium channels; IK, intermediate-conductance calcium-activated potassium channels; AHP, after-hyperpolarization; 1-EBIO, 1-ethyl-2-benzimidazolinone; PCR, polymerase chain reaction; ScTX, scyllatoxin;  $\text{TEA}^+$ , tetraethylammonium; PAC, P1 artificial chromosome; kb, kilobase(s); bp, base pair(s); RT-PCR, reverse transcription-polymerase chain reaction;  $E_{\text{rev}}$ , reversal potential.

modulating dopaminergic transmission, which is hypothesized to be affected in schizophrenia.

Extensive alternative splicing, which increases the functional diversity of channels and allows an optimal adjustment of ion currents to the requirements of certain cells, has been shown for other potassium channels. This was elegantly shown for maxi-K channels in the chicken cochlea (Navaratnam et al., 1997; Rosenblatt et al., 1997; Ramanathan et al., 1999). Thus far, in the SK/IK channels, alternative splicing has only been shown for SK1 in human (Zhang et al., 2001) and mouse (Shmukler et al., 2001). In the latter case, the calmodulin binding site is affected, which indicates that the gating of the channels is altered between SK1 isoforms. However, the newly detected isoform reported in this article, hSK3\_ex4, differs from the previously known hSK3 isoform by an additional extracytosolic loop between the fifth transmembrane helix and the P-loop region. These isoforms are shown to be generated by the alternative skipping of the fourth coding exon. This insertion is shown to alter the pharmacokinetic properties of SK3 channels.

## Materials and Methods

**cDNA Amplification.** cDNA was amplified from a human embryonic cDNA library containing cDNAs from 6-, 7-, and 8-week-old human embryos (a gift from Dr Francis Poullat, Centre National de la Recherche Scientifique, Paris, France) using the PeqLab long-distance PCR system (PeqLab, Erlangen, Germany) and primers F10 (TTTACCCCTCTTCTTTCT) and R11 (GTGGGGAGATTTATTTA). PCR products were gel-purified and cloned using the TOPO-TA kit version D (Invitrogen, Karlsruhe, Germany). Plasmids from 10 clones were sequenced. One clone, SK3-45.1, was used for generating cDNA constructs for expression in mammalian cells.

**Analysis of the Genomic Structure of the hSK3/KCNN3 Gene.** Two cDNA probes, 5'CAG and 3'CAG, on either side of the CAG repeats were generated by PCR from the clone AAD14 (GenBank accession no. Y08263), using the primers F10/R17 (GGGCACTTGGGGTCTTCATC) and F11 (TCCTCTCCCACCGCTT)/R10 (GACACCTTTCCACAGTATG). These probes were used together, thus excluding the CAG repeats from the probe. An additional 3' probe was generated by PCR with the primers R11 (GTGGGGAGATTTATTTA) and F15 (GGGAAAGGTGTCTGTCT), from the IMAGE clone 700710 (GenBank accession no. AA285078). DNA probes were labeled with [<sup>32</sup>P]dCTP by random priming using the Rediprime II kit (Amersham Biosciences Inc., Freiburg, Germany).

P1 artificial chromosome (PAC) clones containing hSK3 were isolated from the human PAC library RPC11,3-5 704 from the Resource Centre of the German Human Genome Project by hybridization with the above three radioactively labeled probes, as described by Church and Gilbert (1985). PACs were subcloned into pUC18 after PstI digestion (Fermentas Inc., St. Leon-Rot, Germany). Clones containing DNA fragments homologous to cDNA sequences were selected by two rounds of hybridization with the same DNA probes described above and were rescreened. Clones found to be positive after both rounds of screening were cultured, and plasmids were analyzed by PstI digestion.

**Alternative Splicing of hSK3.** Plasmids containing only one PstI fragment were sequenced using M13 universal primers and the BigDye cycle sequencing kit (PerkinElmer Life and Analytical Sciences, Rodgau-Juegesheim, Germany). Plasmids harboring PstI fragments longer than 2 kb were shotgun-sequenced using M13 universal primers and the BigDye Cycle-Sequencing kit (PerkinElmer Life and Analytical Sciences). The PstI fragments were concatemerized, random fragments were generated and amplified as described previously (Nehls and Boehm, 1995). Fragments of 0.8 to 1.2 kb were selected by agarose gel electrophoresis and cloned

into TOP10 cells using the TOPO-TA Kit version D (Invitrogen). Plasmids from 20 clones were sequenced as described above.

Vectorette PCR (Riley et al., 1990) was used to amplify anonymous DNA fragments next to fragments with known sequence. Vectorette adapters were obtained by annealing 1 nmol of the oligonucleotides TCCGGTACATGATCGAGGGACTGACAACGAACGAACGGTTGAAGGGAGAGCATG and CTCTCCCTTCTCTAGCGGTAAAACGACGGCCAGTCCTCGATCATGTACCGGA in the presence of 100 mM Tris-HCl, pH 7.4, and 10 mM MgCl<sub>2</sub>. PAC DNA (200–400 ng) was digested with AluI, EcoRV, HaeIII, RsaI, ScaI, and HincII. Vectorette adapters were ligated to the restriction products, and the ligation mix was used for PCR using the following primers KL5 (CTAGCGGTAAAACGACGGCCAGT, vectorette primer); RT-R1 (AAGGCTGGGCTGGTGATTC); P14-seq4 (TTAGTATGTGAGTTGTGAC, for exon 4) and P12-seq6 (ATTTCTTCTGTGCTACTGAC, for exon 7). PCR products were cloned using the TOPO-TA Kit version D (Invitrogen). Five clones were sequenced from each fragment as described above. Exon/intron boundaries were identified by comparison of the cDNA sequences with the genomic sequences obtained from these experiments.

**Real-Time Quantitative RT-PCR.** Human total RNA master panel (BD Biosciences Clontech, Palo Alto, CA) and total RNA isolated from eight human brain tissues, lymph node, and peripheral lymphocyte were used to profile the expression pattern of the hSK3\_ex4 variant using a Prism model 7000 sequence detection instrument (Applied Biosystems, Foster City, CA). Methods follow those described previously (Tomita et al., 2003). Briefly, after DNase digestion, total RNA (2 μg) was used as a template for first-strand cDNA synthesis using random hexamers (TaqMan reverse transcription reagents; Applied Biosystems). Forward and reverse primers and TaqMan fluorescent probes specific for the hSK3\_ex4 transcript were designed by Primer Express version 1.5 (Applied Biosystems). The sequence of the forward primer, annealing to exon 3, was 5'-GACCGTCCGTGTCTGTGAAA-3', and that of the reverse primer, designed to anneal to sequence spanning the exon-intron boundary of exons 4 and 5, was 5'-GGTACCAAGCAGGAAGTGATGAG-3'. The TaqMan fluorescent probe (5'-labeled with 6-carboxyfluorescein, and 3'-labeled with 5-carboxytetramethylrhodamine as a quencher), designed to anneal to sequence in exon 4, was 5'-TCCTGAATCACAGCCAGCCTTC-3'. The hSK3\_ex4 amplification product was 71 bp. Details of the primers and probe used to define SK3 have been described previously (Tomita et al., 2003). To obtain quantification of absolute message abundance, standard curves were plotted for every assay, and each was generated using eight different concentrations of an hSK3\_ex4 construct in pcDNA4\_HisMax-TOPO. Each experiment was carried out in triplicate.

**cDNA Constructs for Mammalian Expression.** The entire open reading frame of hSK3\_ex4 was amplified from clone SK3-45.1 with Pfu-polymerase using the primers SK3-F1 (AAAACTCGAGC-CACCATGGACACTTCTGGGCACTTC) and SK3-R1 (AAAATG-GATCCCCGCAACTGCTTGAACCTTGTTGA). After cloning the fragment using the TOPO-TA kit (Invitrogen) as described above, the PCR product was confirmed by sequencing. A partial cDNA fragment was excised using enzymes HindIII and SfiI and was cloned into the plasmid pHygroSK3-Q19 (a kind gift from Dr. H. Jäger, Institute of Applied Physiology, Ulm, Germany). A construct was obtained encoding hSK3\_ex4 with 12 and 19 glutamines in its N-terminal cytosolic region.

**Cell Culture.** tsA cells were cultured in minimal essential medium containing glutamax-I and Earle's salts (Invitrogen, Karlsruhe, Germany) and 10% fetal bovine serum. One to two days before transfection, cells were transferred to a 35-mm Petri dish and were grown to 70% confluence. A mixture of 0.5 μg of plasmid DNA encoding pEGFP-N1 (BD Biosciences Clontech) and 2 μg of plasmid DNA encoding one of the hSK3 isoform was transfected into tsA cells using FUGENE 6 (Roche Applied Science, Mannheim, Germany) according to the manufacturer's protocol. Cells were used for measurements 2 to 4 days after transfection.

**Concentration-Response of hSK3 Isoforms to Apamin, Scylatoxin, *d*-Tubocurarine, TEA<sup>+</sup>, and Ba<sup>2+</sup>.** Experiments were carried out using the whole-cell recording mode of the patch-clamp technique (Hamill et al., 1981). Electrodes were pulled from glass capillaries in three stages and fire-polished to resistances of 3.5 to 4 M $\Omega$  when filled with internal solution (135 mM potassium aspartate, 2 mM MgCl<sub>2</sub>, 10 mM HEPES, 10 mM EGTA, and 8.7 mM CaCl<sub>2</sub> corresponds to [Ca<sup>2+</sup>]<sub>free</sub> of 1  $\mu$ M, pH 7.2). Membrane currents were measured with an EPC-9 amplifier (HEKA Elektronik, Lambrecht/Pfalz, Germany) using Pulse and Pulsefit (HEKA Elektronik) as acquisition and analysis software. The cytosolic Ca<sup>2+</sup> concentration was adjusted to [Ca<sup>2+</sup>]<sub>free</sub> = 1  $\mu$ M by whole-cell dialysis with internal solution. N-Ringer (160 mM NaCl, 4.5 mM KCl, 2 mM CaCl<sub>2</sub>, 1 mM MgCl<sub>2</sub>, and 5 mM HEPES, pH 7.4), K-Ringer (164.5 mM KCl, 2 mM CaCl<sub>2</sub>, 1 mM MgCl<sub>2</sub>, and 5 mM HEPES, pH 7.4), and TEA-Ringer (164.5 mM tetraethylammonium-Cl, 2 mM CaCl<sub>2</sub>, 1 mM MgCl<sub>2</sub>, and 5 mM HEPES, pH 7.4) were used as external solutions.

Membrane potentials were clamped to -160 or -120 mV for 50 ms followed by 400-ms ramps from -160 or -120 to +60 mV and were kept for 5 s between ramps at -80 mV in N-Ringer,  $\pm$ 0 mV in K-Ringer, and -25 mV in K30-Ringer (30 mM KCl, 134.5 mM NaCl, 2 mM CaCl<sub>2</sub>, 1 mM MgCl<sub>2</sub>, 5 mM HEPES, pH 7.4) as external solution. All potentials caused by the liquid junction potential that develops at the tip of the pipette if the pipette solution is different from that of the bath were less than 5 mV and were therefore not corrected for. TEA<sup>+</sup>, Ba<sup>2+</sup>, apamin, ScTX, *d*-tubocurarine, and 1-EBIO were added to the external solution in increasing concentrations. Curves were fitted using the software Slide Writer Plus version 4.1 (Advanced Graphics Software Inc., Encinitas, CA).

**Selectivity of hSK3 and hSK3\_ex4 to Monovalent Cations.** Patch-clamp recordings were carried out after whole-cell dialysis with internal solution as described above. The membrane potential was clamped to -120 mV for 50 ms followed by a 400-ms ramp from -120 to +60 mV. K-Ringer, TEA-Ringer, K0-Ringer (164.5 mM NaCl, 2 mM CaCl<sub>2</sub>, 1 mM MgCl<sub>2</sub>, and 5 mM HEPES, pH 7.4), Rb-Ringer (164.5 mM RbCl, 2 mM CaCl<sub>2</sub>, 1 mM MgCl<sub>2</sub>, and 5 mM HEPES, pH 7.4), and Cs-Ringer (164.5 mM CsCl, 2 mM CaCl<sub>2</sub>, 1 mM MgCl<sub>2</sub>, and 5 mM HEPES, pH 7.4) were used as external solutions. Liquid junction potentials for K0-Ringer, Rb-Ringer, Cs-Ringer, and TEA-Ringer were less than 5 mV and were therefore not corrected for.

**Activation of hSK3 and hSK3\_ex4 by Intracellular Ca<sup>2+</sup>.** Experiments were carried out using the whole-cell mode of the patch-clamp technique as described above combined with fura-2 measurements. Light from a 75-W xenon arc lamp was filtered with 10-nm bandwidth filters at wavelengths of 350 nm (F1) and 380 nm (F2) using a filter wheel and a shutter (Lambda 10-2 with fura extension; HEKA Elektronik) under control of the patch-clamp program (Pulse with fura extension, HEKA Elektronik). Emitted light was filtered at 515 nm with a bandwidth of 15 nm, and its intensity was measured using the T.I.L.L. photometry system (Photonics, Pittsfield, MA). Autofluorescence was measured from single cells before each experiment. For calibration, tsA cells transiently transfected with dsRED (BD Biosciences Clontech) were perfused with internal solution containing 0, 0.1, 0.4, 0.6, 1.0, 1.3, 1.5, 1.8, 2.0, 5.0, and 39.0  $\mu$ M [Ca<sup>2+</sup> concentrations were calculated using CaCLV 2.2 (Fohr et al., 1993)] and 200  $\mu$ M fura-2 (Molecular Probes, Eugene, OR). N-Ringer with symmetrical Ca<sup>2+</sup> concentrations was used as external solution. Currents were elicited by clamping the membrane potential to -120 mV followed by 2-s ramps from -120 to +60 mV. Between each ramp, the potential was clamped at -80 mV for 3 s. The intensity of the emitted light was measured during each ramp (F1 and F2 for 200 ms each), and the intensity of the autofluorescence light was subtracted for each wavelength separately. Ratios were calculated according to  $R = F1/F2$  and plotted against the Ca<sup>2+</sup> concentrations. After curve-fitting according to the equation  $R = ([Ca^{2+}] \times R_{max} + K_d \times R_{min}) / ([Ca^{2+}] + K_d)$  using Slide Writer Plus 4.1 (Advanced Graphics Software Inc.) values for  $K_d$ ,  $R_{max}$ , and  $R_{min}$  were calculated to be 1.63

$\mu$ M, 2.2, and 0.21, respectively. For measuring the calcium dependence of hSK3 and hSK3\_ex4, tsA cells were transfected with the cDNA constructs described above together with dsRED as transfection marker. Measurements were carried out 3 to 4 days after transfection. Pipettes were pulled as described and were filled with 2 to 4  $\mu$ l of tip solution (200  $\mu$ M fura-2, 135 mM potassium aspartate, 1 mM MgCl<sub>2</sub>, 10 mM HEPES, 1 mM EGTA, and 0.92 mM CaCl<sub>2</sub> corresponding to 2  $\mu$ M free Ca<sup>2+</sup>, pH 7.2), which was overlaid with pipette solution (200  $\mu$ M fura-2, 135 mM potassium aspartate, 1 mM MgCl<sub>2</sub>, 10 mM HEPES, 10 mM EGTA, and 0 mM CaCl<sub>2</sub>, pH 7.2). K-Ringer was used as bath solution, and whole-cell currents were measured after perfusion of cells in parallel to the fura measurements.

## Results

**Alternative Splicing.** We were able to amplify and clone a 2.5-kb transcript of hSK3 from a human embryonic cDNA library derived from human embryos aged 6, 7, and 8 weeks using primers that flank the entire open-reading frame of hSK3 (primers F10 and R11). Ten clones were initially analyzed by end-sequencing and were identified as clones containing cDNAs from hSK3. Sequencing of the entire inserts of two of these clones indicated that they both contained 19 CAGs in the second repeat and a 45-bp insertion between nucleotide positions 1463 and 1464 (Fig. 1) within the codon Arg488, which results in the amino acid change R488S. The insertion does not disturb the open reading frame and codes for the 15 amino acids PESPAQPSGSSLPAAW (Fig. 1) in the extracytosolic region between the fifth transmembrane helix and the P-loop region. Neither AAD14 nor the IMAGE clone 700710, which was used to construct the hSK3 cDNA, contains the 45-bp insertion (Chandy et al., 1998).

**Analysis of the Genomic Structure of the Human hSK3/KCNN3 Gene.** To confirm that the newly detected hSK3 transcript originated from the hSK3/KCNN3 gene, we looked for the 45-bp insert sequence on genomic DNA clones spanning the hSK3/KCNN3 gene. Screening of the human PAC DNA library using two DNA probes that flanked the CAG repeats revealed 13 overlapping PAC clones containing parts of the hSK3 gene. Two PACs, LLNLP704G20940Q3 (P12) and LLNLP704G23676Q3 (P14), were subcloned, and six subclones, each containing a single PstI fragment, were sequenced. The corresponding genomic sequence of the 45-bp insert, which was found in the PCR product derived from the human embryonic cDNA library, was determined from a cloned fragment of PAC P14 obtained by vectorette PCR. As shown in Fig. 1C, the 45-bp sequence is flanked by typical splice acceptor and donor sequences and was also found in the genomic sequence AF336797 extending from position 134161 to 134205. This confirms that the 45-bp insert represents an additional exon, which is spliced between the previously designated third and fourth coding exons (Sun et al., 2001), and we have therefore numbered it exon 4.

**hSK3\_ex4 Is Expressed Widely.** TaqMan quantitative RT-PCR was used to determine the abundance of hSK3 and hSK3\_ex4 transcripts in total RNA derived from 29 human tissues. We have arbitrarily divided the expression levels for hSK3 into three groups (defined by horizontal lines in Fig. 2), abundant (>10,000 copies/ $\mu$ l cDNA), intermediate (100–10,000 copies/ $\mu$ l cDNA), and low (<100 copies/ $\mu$ l cDNA). Consistent with previous reports (Rimini et al., 2000; Tomita et al., 2003), hSK3 is expressed abundantly in brain, striated and smooth muscle, spleen, thymus, adrenal, thy-

roid, prostate, kidney, and testis. It is expressed at intermediate levels in heart, lymph node, bone marrow, fetal liver, salivary gland, liver, lung, and placenta and at low levels in peripheral lymphocytes (Fig. 2). hSK3\_ex4 is present at an intermediate level in most of the brain regions examined, as well as in striated and smooth muscles, thymus, thyroid, testis, bone marrow, spleen, lymph node, and peripheral lymphocytes. It is expressed at lower levels in all of the other tissues studied (Fig. 2). The expression level of hSK3\_ex4 tends to parallel that of the hSK3 transcript, and it is generally at a level 0 to 2% of that of hSK3. An exception, however, is found in peripheral lymphocytes, in which the ratio of hSK3\_ex4/hSK3 is exceptionally high. This is brought about not by an increase in the absolute abundance of hSK3\_ex4, but rather it reflects the exceptionally low expression of hSK3 in this tissue.

**Functional Characterization of hSK3 Isoforms.** Because the newly detected hSK3 isoform differs in the S5 to P-loop region, we were interested in whether this alteration affects its pharmacological and kinetic properties. Therefore, we tested the effect of blockers, which are known to bind to the outer pore region of SK channels, such as TEA<sup>+</sup>, *d*-tubocurarine, apamin, and ScTX, a toxin isolated from the scorpion *Leiurus quinquestriatus hebraeus*, which is also re-

ported as leiurotoxin I (Chicchi et al., 1988), as well as the effect of Ba<sup>2+</sup>, which is known to bind to the inner vestibule of SK channels. We also determined the fractional permeability of the monovalent cations Rb<sup>+</sup>, Cs<sup>+</sup>, and Na<sup>+</sup> in comparison to K<sup>+</sup> and the activation of the isoforms by 1-EBIO.

**Apamin.** We used apamin as a classic peptidic SK-channel blocker. Apamin is shown to bind to the outer pore region of SK channels (Ishii et al., 1997). Representative experiments for both isoforms are shown in Fig. 3, A and B. In these experiments, the membrane potential was ramped from -120 to +60 mV. In these experiments, an almost linear current/voltage relationship was observed for membrane potentials that were more negative than -40 mV. The slope conductance was determined for the interval between -90 and -70 mV. For cells expressing isoform hSK3, the slope conductance was found to be  $0.5 \pm 0.5$  nS ( $n = 5$ ) in N-Ringer solution. After changing the external solution to K-Ringer, an elevated inward current was observed at negative potentials. The current/voltage relationship of this current was also linear for membrane potentials more negative than -40 mV. The slope conductance for the above-mentioned interval was elevated to  $12.3 \pm 22.3$  nS ( $n = 5$ ). Apamin was added to K-Ringer as external solution in increasing concentrations of 0.1, 1, 5, 10, and 100 nM. A voltage-independent but concen-

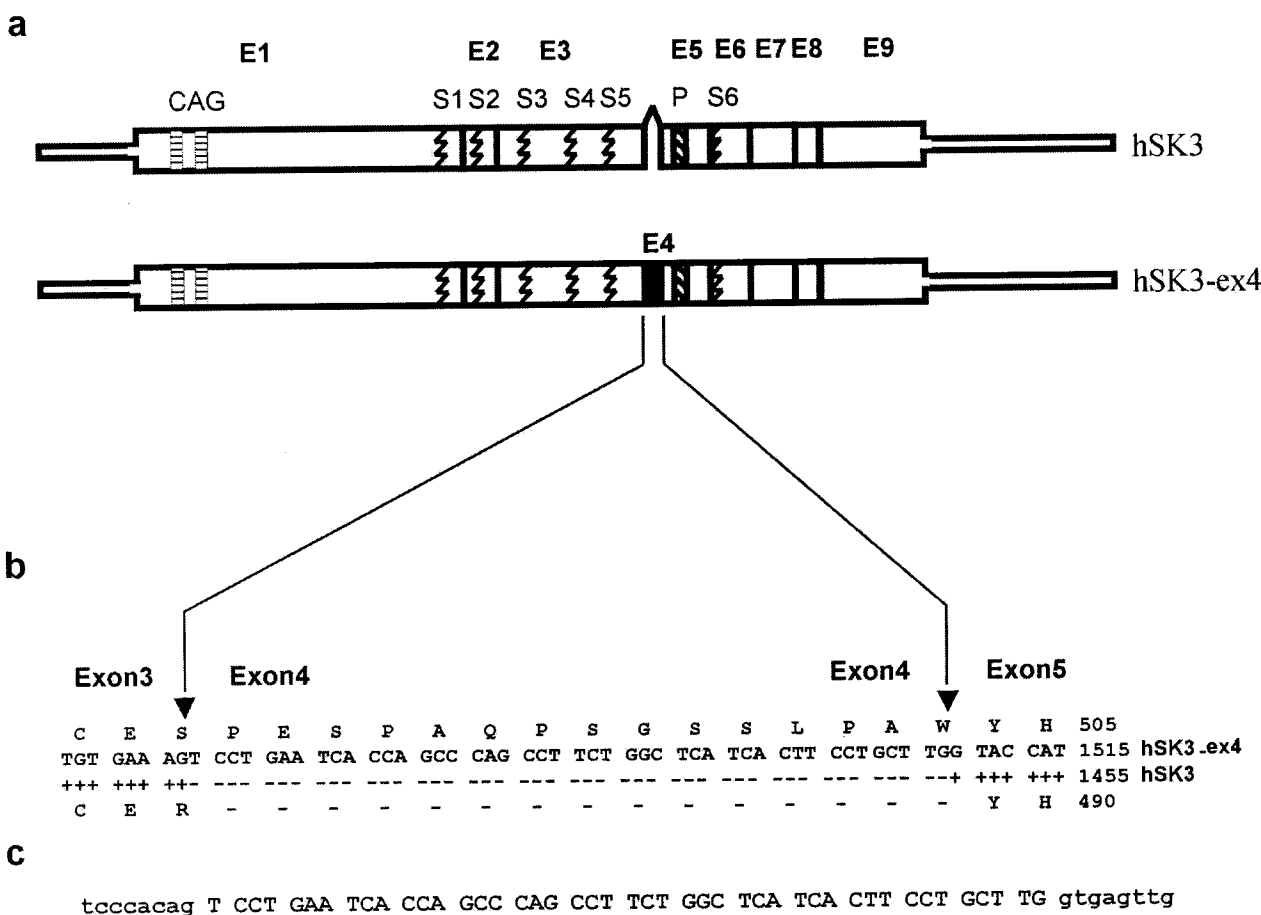


**Fig. 1.** Comparison of hSK3 and hSK3\_ex4 cDNAs. A, a schematic alignment of both cDNAs. Narrow boxes represent 3' and 5' untranslated regions, and broad boxes indicate the coding region. Exon boundaries are shown as straight lines, and the exons are given above as E1 to E9. Both CAG repeats are lying in the coding region of the first exon (E1). The transmembrane helices S1 to S6 are delineated by jagged lines, and the P-loop (P) is shown as a diagonally shaded box. Exon 4 (E4) is shown as a filled black box. B, the alignment of the surrounding region of exon 4 shown in more detail. The nucleotide sequences of both transcripts are given. Amino acid sequences of both isoforms are shown as a single-letter code above and below each nucleotide sequence. -, lacking residues; +, identical nucleotides; arrowheads, exon boundaries. C, the splice-acceptor and splice donor sequences surrounding exon 4. Noncoding sequences are shown in lowercase letters, whereas the coding region is shown in uppercase letters.

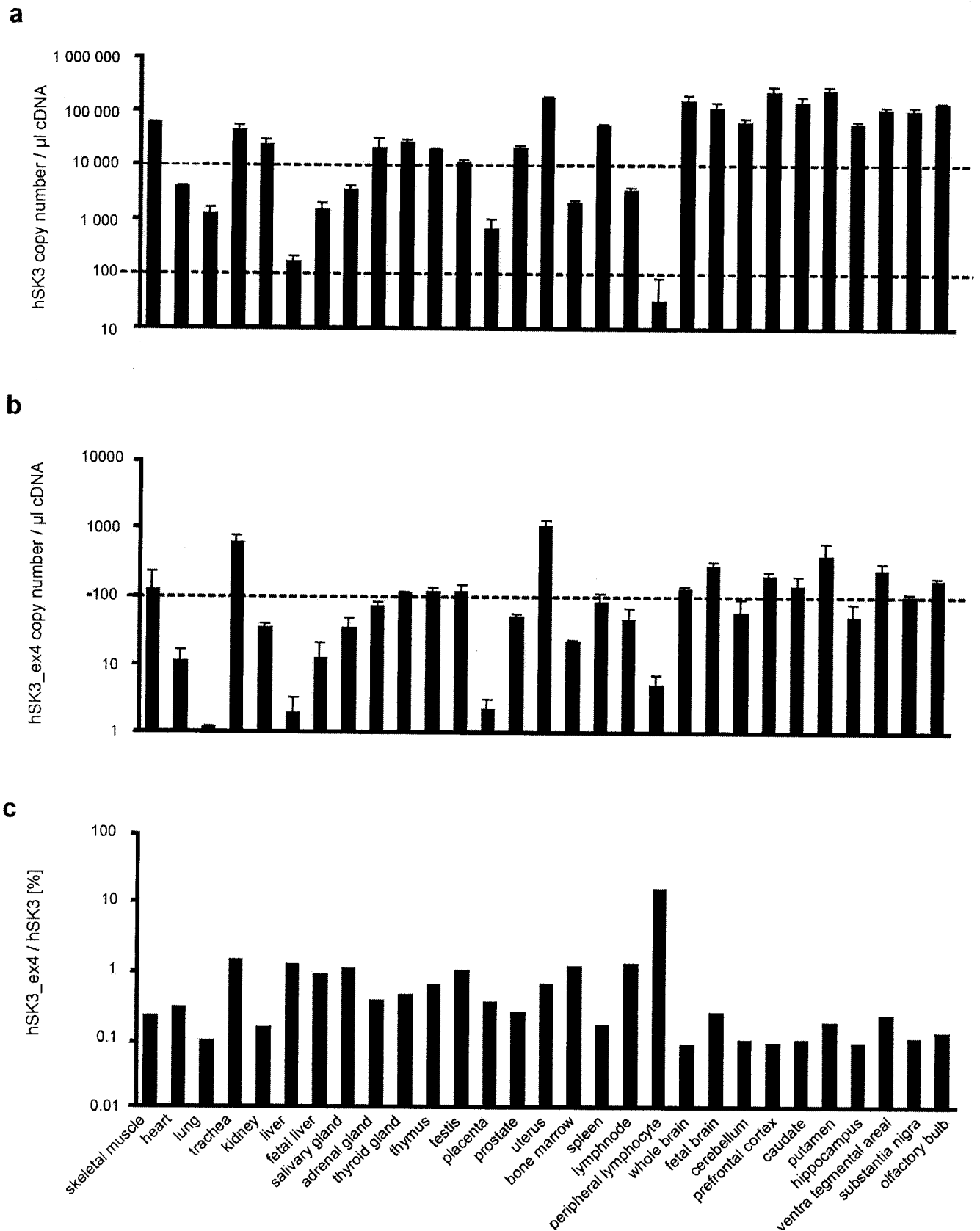


**Fig. 2.** Tissue distribution of hSK3 and hSK3\_ex4 transcripts. The total number of transcripts in 1  $\mu$ l of cDNA solution is shown in A (for hSK3) and B (for hSK3\_ex4). Expression levels are grouped into abundant (>10,000 copies/ $\mu$ l cDNA), intermediate (100–10,000 copies/ $\mu$ l cDNA), and low (<100 copies/ $\mu$ l cDNA). Horizontal broken lines indicate the threshold between low and intermediate expression levels. C, the ratio of hSK3\_ex4 to hSK3 transcripts in percentage of hSK3.

tration-dependent blockage of currents was observed, which was carried by hSK3. At a concentration of 100 nM apamin (in K-Ringer as external solution), the remaining whole-cell conductance was found to be  $0.8 \pm 0.6$  nS ( $n = 5$ ), which corresponds to a reduction of the whole-cell conductance of approximately 94%. The calculated  $K_d$  value was found to be 0.8 nM, which is in good agreement with previously published  $K_d$  values for SK3 channels of 0.63 nM (Grunnet et al., 2001b) using similar electrophysiological methods. A higher  $K_d$  value of 13.2 nM was reported by Terstappen et al. (2001) using fluorescence techniques. In the case of isoform hSK3\_ex4-expressing cells, the slope conductances in

N-Ringer and K-Ringer solutions were found to be  $0.8 \pm 0.8$  nS ( $n = 6$ ) and  $3.8 \pm 2.5$  nS ( $n = 6$ ), respectively. After adding 100 nM apamin to K-Ringer as external solution, the remaining whole-cell conductance was found to be  $4.3 \pm 3.0$  nS ( $n = 6$ ). Therefore, whole-cell currents, which were carried by hSK3\_ex4, remain unaffected by 100 nM apamin. Therefore, hSK3\_ex4 channels are more insensitive to apamin than SK1 channels, which were reported to be the most insensitive SK channels with a  $K_d$  value of 196 nM (Grunnet et al., 2001a).

**Scyllatoxin.** Representative experiments for both isoforms are shown in Fig. 4, A and B. N-Ringer and K-Ringer were used as external solutions. Membrane potentials were

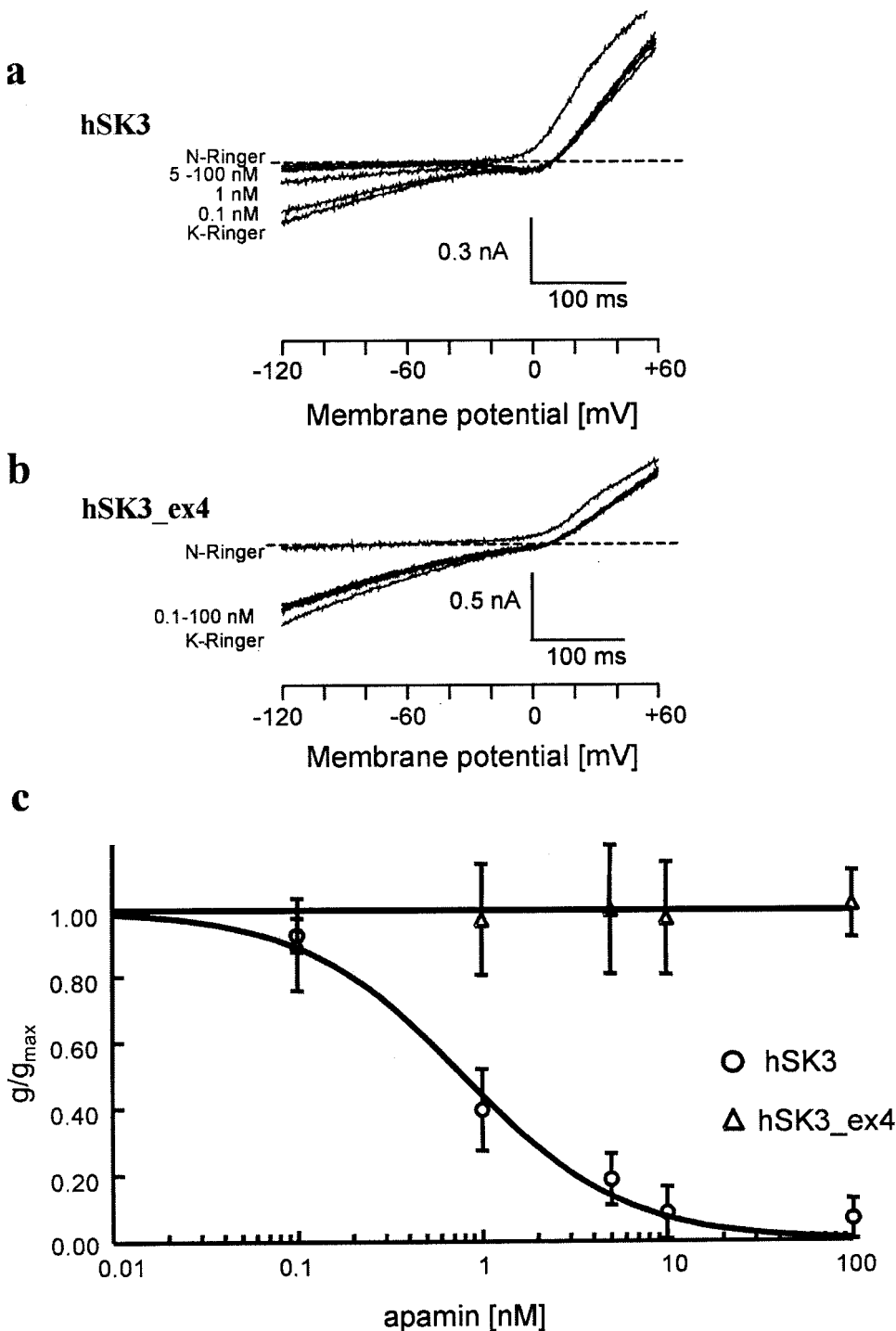


**Fig. 3.** Effect of apamin on current through hSK3 and hSK3\_ex4. A and B show the whole-cell ramp currents for hSK3 and hSK3\_ex4 elicited by clamping the membrane potentials in 400-ms ramps from  $-120$  to  $+60$  mV in N-Ringer and K-Ringer solutions with and without different concentrations of apamin (concentrations given at the left of each trace). C, dose-response curve for experiments similar to those shown in A and B. Whole-cell currents, which were measured in N-Ringer as external solution, were subtracted from currents measured in K-Ringer with and without apamin. The ratio of the whole-cell conductance observed in toxin-containing solution was obtained by measuring the slope of the ramp current between  $-90$  and  $-70$  mV, divided by the whole-cell conductance in K-Ringer as external solution and plotted against the apamin concentration. Error bars represent the standard deviation. The solid lines through the data points (○, hSK3; △, hSK3\_ex4) are the best fits to the data of a Hill equation according to  $g/g_{\max} = 1/(1 + [\text{apamin}]/K_d)$ , assuming a Hill coefficient of 1. Dissociation constants were calculated to be 0.8 nM for hSK3. A  $K_d$  value for hSK3\_ex4 was not calculated because no reduction of whole-cell conductance can be observed up to 100 nM apamin.

ramped from  $-160$  to  $+60$  mV for 400 ms. The slope conductance determined for the interval between  $-90$  to  $-70$  mV with N-Ringer as external solution was  $1.9 \pm 1.2$  nS ( $n = 11$ ) for hSK3 and  $2.4 \pm 1.4$  nS ( $n = 9$ ) for isoform hSK3\_ex4. In K-Ringer solution, the slope conductance increased to  $11.4 \pm 3.7$  nS ( $n = 11$ ) and  $15.0 \pm 5.7$  nS ( $n = 9$ ) for hSK3 and hSK3\_ex4, respectively, when the external solution was re-

placed by K-Ringer. After scyllatoxin was added in increasing concentrations of 0.1, 1, 5, 10, 50, and 100 nM (and 500 nM in the case of hSK3\_ex4) to K-Ringer, the current, which was carried through hSK3 was blocked in a voltage-independent but concentration-dependent manner with a  $K_d$  value calculated to be 2.1 nM (Fig. 4C, solid line). This finding is in line with a previous study, which determined a  $K_d$  of 1 nM for the

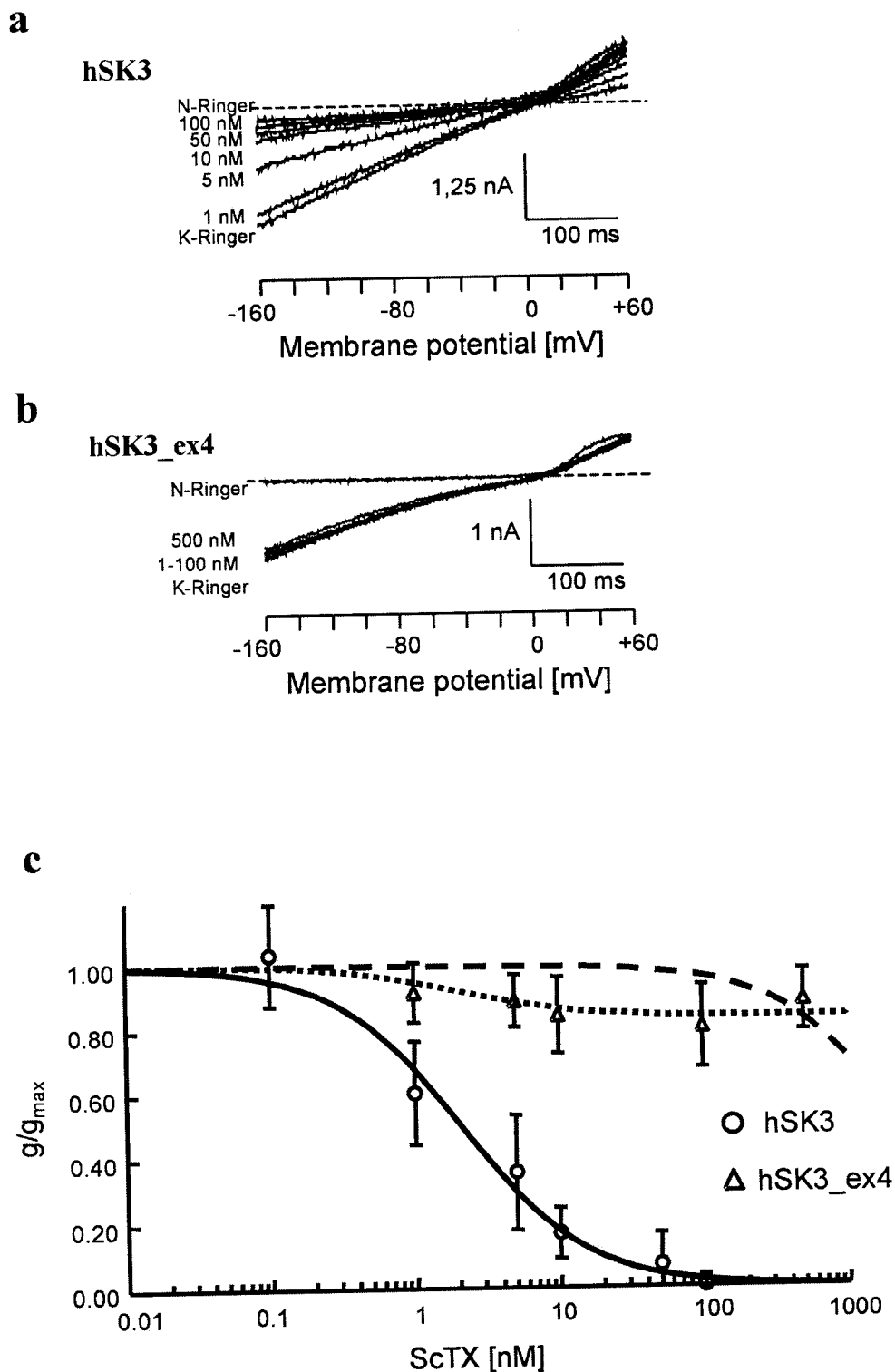


**Fig. 4.** Effect of ScTX on current through hSK3 and hSK3\_ex4. A and B, the whole-cell ramp currents for hSK3 and hSK3\_ex4 elicited by clamping the membrane potentials in 400-ms ramps from  $-160$  to  $+60$  mV in N-Ringer and K-Ringer with and without different concentrations of ScTX (concentrations are given at the left of each trace). C, dose-response curve for experiments similar to those shown in A and B. Whole-cell currents, which were measured in N-Ringer as external solution, were subtracted from currents measured in K-Ringer with and without ScTX. The ratio of the whole-cell conductance observed in toxin-containing solution was obtained by measuring the slope of the ramp current between  $-90$  and  $-70$  mV, divided by the whole-cell conductance in K-Ringer as external solution, and plotted against the ScTX concentration. Error bars represent the standard deviation. The solid (hSK3) and dashed (hSK3\_ex4) lines through the data points are the best fits to the data of a Hill equation according to  $g/g_{\max} = 1/(1 + [\text{ScTX}]/K_d)$ , assuming a Hill coefficient of 1. Dissociation constants were calculated to be 2.1 nM for hSK3 and  $2.6 \mu\text{M}$  for hSK3\_ex4. The dotted (hSK3\_ex4) lines through the data points are the best fits of a modified Hill equation according to  $g/g_{\max} = 1 - (a/(1 + K_d/[\text{ScTX}]))$ , assuming a  $K_d$  identical with that found for hSK3 (2.1 nM) and a Hill coefficient of 1. The calculated maximal inhibition of current was found to be  $a = 16.7\%$ .

ScTX block of hSK3 (Shakkottai et al., 2001). In contrast, the current carried by isoform hSK3\_ex4 remains almost unaffected by scyllatoxin. Only an approximately 12% reduction of whole-cell conductance was observed for a concentration of 500 nM of ScTX (Fig. 4C). A  $K_d$  of 2.6  $\mu$ M was calculated for hSK3\_ex4, assuming a blocking mechanism identical with that for hSK3 (Fig. 4C, dashed line). We are aware that this calculation can only be an estimate of the minimal  $K_d$  value, because we only measured block of current by ScTX up to 500 nM. On the other hand, we can also describe the data assuming an identical  $K_d$  compared with hSK3 but with a maximal inhibition of only 16.7% (Fig. 4C, dotted line). Independent of the inhibition mechanism, it is obvious that the current through this isoform is hardly reduced by the presence of

even 500 nM ScTX in contrast to the SK1 channel, which has been shown to be the most insensitive member of the SK channel family, with a  $K_d$  for ScTX of 80 (Strobaek et al., 2000) and 325 nM (Shakkottai et al., 2001).

***d*-Tubocurarine.** The effect of *d*-tubocurarine on current through the hSK3 and hSK3\_ex4 is shown in representative experiments in Figs. 5, A and B. Membrane potentials were ramped from  $-120$  to  $+60$  mV for 400 ms. The slope conductance calculated for the interval from  $-90$  to  $-70$  mV was found to be  $1.4 \pm 1.5$  nS ( $n = 4$ ) and  $0.7 \pm 0.4$  nS ( $n = 4$ ) with N-Ringer as external solution for hSK3 and hSK3\_ex4, respectively. After changing the bath solution to K-Ringer, an increased whole-cell conductance of  $9.6 \pm 9.8$  nS (hSK3) and  $3.7 \pm 1.6$  nS (hSK3\_ex4) was observed. *d*-Tubocurarine was

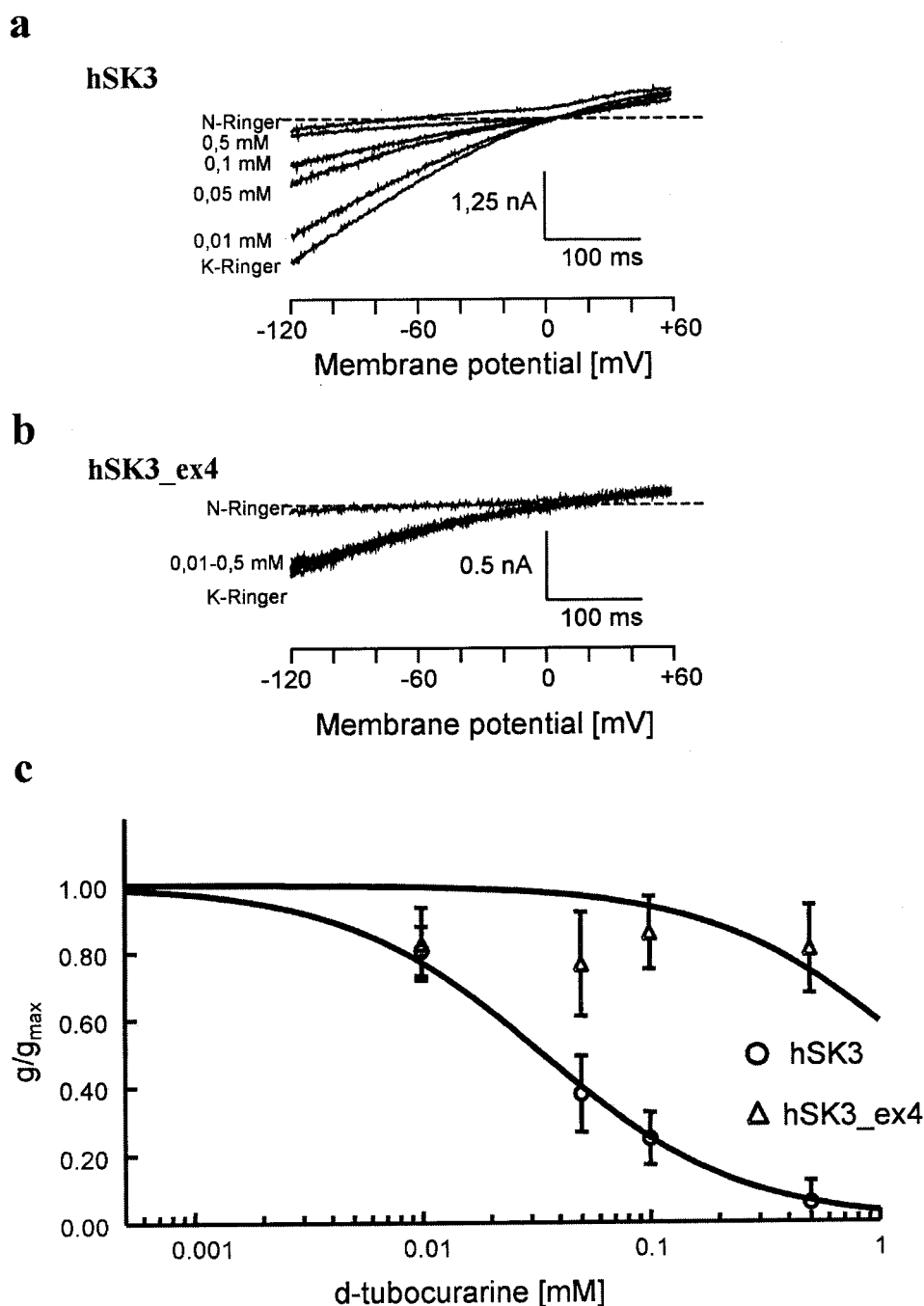


**Fig. 5.** Effect of *d*-tubocurarine on current through hSK3 and hSK3\_ex4. A and B, whole-cell ramp currents for hSK3 and hSK3\_ex4 elicited by clamping the membrane potentials in 400-ms ramps from  $-120$  to  $+60$  mV in N-Ringer and K-Ringer solutions with and without different concentrations of *d*-tubocurarine (concentrations are given at the left of each trace). Whole-cell currents, which were measured in N-Ringer as external solution, were subtracted from currents measured in K-Ringer with and without *d*-tubocurarine. The ratio of the whole-cell conductance observed in toxin-containing solution was obtained by measuring the slope of the ramp current between  $-90$  and  $-70$  mV, divided by the whole-cell conductance in K-Ringer as external solution, and plotted against the *d*-tubocurarine concentration. Error bars represent the standard deviation. The curves through the data points are the best fits of a Hill equation to the data according to  $g/g_{\max} = 1/(1 + [d\text{-tubocurarine}]/K_d)$ , assuming a Hill coefficient of 1. Dissociation constants were calculated to be 33.4  $\mu$ M for hSK3 and 1.4 mM for hSK3\_ex4 with the assumption that the blocking mechanism is the same for both isoforms.

added to the bath in increasing concentrations of 10, 50, 100, and 500  $\mu\text{M}$ . Currents carried by the hSK3 isoform were blocked in the presence of *d*-tubocurarine in a voltage-independent and concentration-dependent manner. In the presence of 500  $\mu\text{M}$  *d*-tubocurarine, 95% of the current carried by isoform hSK3 was blocked, whereas currents carried by hSK3\_ex4 were reduced by only approximately 20%. Concentration-response curves were fitted as described for ScTX (Fig. 5C). The  $K_d$  observed for isoform hSK3 was 33.4  $\mu\text{M}$ , which is between those previously observed for SK1 ( $K_d = 354.3 \mu\text{M}$ ) and SK2 ( $K_d = 5.4 \mu\text{M}$ ) (Ishii et al., 1997). Only if identical blocking mechanisms are assumed for both isoforms, a  $K_d$  of 1.4 mM can be calculated for isoform hSK3\_ex4. It is also possible to assume an incomplete *d*-tubocurarine block for hSK3\_ex4 similar to that one discussed for the ScTX block shown in Fig. 4C.

**TEA<sup>+</sup> Block.** Measurements were carried out with N-Ringer and K-Ringer as external solutions, and membrane potentials were clamped in 400-ms ramps from  $-120$  to  $+60$  mV. An almost linear potassium current was observed for membrane potentials more negative than  $-40$  mV with N-Ringer as external solution; this was elevated as described above when the external solution was exchanged with K-Ringer. TEA<sup>+</sup> was added to K-Ringer in increasing concentrations of 0.1, 0.5, 1, 5, and 10 mM. In contrast to the scyllatoxin block, TEA<sup>+</sup> has a similar effect on hSK3- as well as hSK3\_ex4-carried currents, and the calculated dissociation constants were similar for both isoforms ( $K_d = 2.2$  mM for hSK3 and 2.6 mM for hSK3\_ex4).

**External Ba<sup>2+</sup> Block.** To test whether the additional 15 amino acids also affect the inner vestibule of the pore, we investigated the inhibition of both isoforms by external Ba<sup>2+</sup> (Fig. 6). For both isoforms, the number of experiments was  $n = 3$ . K-Ringer and TEA-Ringer were used as external solutions, and BaCl<sub>2</sub> was added to K-Ringer in increasing concentrations of 0.1, 0.5, and 1 mM. The membrane potential was clamped in 400-ms ramps from  $-160$  to  $+60$  mV. This is an appropriate protocol because it has already been shown that the Ba<sup>2+</sup> block is fast compared with the voltage ramp (Hanselmann and Grissmer, 1996). Whole-cell currents with TEA-Ringer as external solution were assumed to be leak currents and were therefore subtracted from the whole-cell currents in K-Ringer with and without Ba<sup>2+</sup>. Relative currents were calculated as fractions of the currents with K-Ringer as external solution. The potassium currents through both isoforms were affected by external Ba<sup>2+</sup> in a concentration-dependent manner (Fig. 6). However, the blockage was strongest at hyperpolarized potentials and was reversible immediately after washout. To analyze the voltage-dependence of the Ba<sup>2+</sup> block, the relative currents for each Ba<sup>2+</sup> concentration were plotted against the membrane potential ranging from  $-160$  mV to  $-40$  mV, and curves were fitted according to the Boltzmann equation  $I/I_{\text{K-Ringer}} = 1/(1 + \exp((E_{0.5} - E)/k))$  with  $k$  as the steepness factor of block (Fig. 6, C and D). The calculated half-maximal blocking potentials ( $E_{0.5}$  values) were  $-160 \pm 4$  mV (0.1 mM Ba<sup>2+</sup>),  $-117 \pm 2$  mV (0.5 mM Ba<sup>2+</sup>), and  $-91 \pm 9$  mV (1 mM Ba<sup>2+</sup>) for hSK3 ( $n = 3$ ). For hSK3\_ex4 ( $n = 3$ ), the values were calculated to be  $-290 \pm 145$  mV (0.1 mM Ba<sup>2+</sup>),  $-186 \pm 17$  mV (0.5 mM Ba<sup>2+</sup>), and  $-146 \pm 17$  mV (1 mM Ba<sup>2+</sup>). The strongly increased standard deviation, which was calculated for  $E_{50}$  at 0.1 mM Ba<sup>2+</sup> of hSK3\_ex4, is caused by the reduced

steepness of the voltage dependence of the Ba<sup>2+</sup> block. The steepness factors calculated for hSK3 and hSK3\_ex4 were  $32 \pm 4$  and  $61 \pm 12$  mV, respectively. This corresponds to Ba<sup>2+</sup>-binding sites at fractions of  $\delta = 0.42$  from the outside of the electrical field for hSK3 and  $\delta = 0.23$  for hSK3\_ex4. Therefore, the Ba<sup>2+</sup>-binding site calculated for both isoforms is less deep than the one reported for the apamin-sensitive ( $\delta = 0.62$ ) and charybdotoxin-sensitive ( $\delta = 0.74$ ) potassium channels in Jurkat E6-1 cells and human peripheral T lymphocytes (Hanselmann and Grissmer, 1996). However, the data obtained for hSK3 indicate that Ba<sup>2+</sup> binds to residues at the inner vestibule of the pore and that the hSK3\_ex4 isoform has a different Ba<sup>2+</sup>-binding site, which seems to be shifted toward the outside of the vestibule.

**Selectivity of hSK3 Isoforms to Monovalent Cations.** Because the altered Ba<sup>2+</sup>-binding site in the hSK3 isoform is approximately halfway into the electrical field of the channel one could assume that the conduction pathway and possibly the selectivity filter might be altered as well. Therefore, we investigated the selectivity of the hSK3 isoforms to different monovalent cations (Fig. 7). The whole-cell current in the presence of TEA-Ringer was assumed to be leak current and was subtracted from the whole-cell currents in the presence of K-Ringer, Rb-Ringer, Cs-Ringer, and K0-Ringer (contains 164.5 mM Na<sup>+</sup> without K<sup>+</sup>). The reversal potential ( $E_{\text{rev}}$ ) was found to be  $12 \pm 2$  mV in K-Ringer,  $-115 \pm 24$  mV in K0-Ringer,  $6 \pm 2$  mV in Rb-Ringer, and  $-33 \pm 7$  mV in Cs-Ringer for hSK3 ( $n = 6$ ). For isoform hSK3\_ex4 ( $n = 5$ ),  $E_{\text{rev}}$  was found to be  $13 \pm 4$  mV in K-Ringer,  $-114 \pm 39$  mV in K0-Ringer,  $6 \pm 1$  mV in Rb-Ringer, and  $-34 \pm 4$  mV in Cs-Ringer. The positive reversal potentials found, especially in K-Ringer, are because the currents were not corrected for junction potentials. For both isoforms, the number of experiments was  $n = 3$ . Because the slope of the current ramps obtained from the experiments in K0-Ringer was very small (slope conductance  $g < 0.1$  nS for both isoforms), the estimated  $E_{\text{rev}}$  varied strongly, and therefore data were not shown. The relative permeabilities were calculated from  $E_{\text{rev}}$  as described previously (Hille, 2001) and are given together with the relative conductances in Table 1 as fractions of the permeability and conductance of both isoforms for K<sup>+</sup>. However, both isoforms show similar relative permeabilities for Cs<sup>+</sup> and Rb<sup>+</sup>. Only the relative conductance for Rb<sup>+</sup> was found to be higher for hSK3 ( $g_{\text{Rb}}/g_{\text{K}} = 1.1$ ) than for hSK3\_ex4 ( $g_{\text{Rb}}/g_{\text{K}} = 0.77$ ). As already shown for other SK/IK channels (Hanselmann and Grissmer, 1996; Jensen et al., 1998), hSK3 and hSK3\_ex4 can carry a significant Cs<sup>+</sup> current.

**Activation of hSK3 Isoforms by 1-EBIO.** To determine the activation of hSK3 isoforms by 1-EBIO, we carried out experiments in K30-Ringer (contains 30 mM K<sup>+</sup>) as external solution. This prevents leakage of the cells, especially after application of higher concentrations of 1-EBIO to the external solution. The membrane voltage was clamped in 400-ms ramps from  $-120$  to  $+60$  mV. 1-EBIO was added in increasing concentrations of 0.01, 0.1, 0.2, 0.5, and 1 mM to K30-Ringer (Fig. 8, A and B). The slope conductance was calculated for the interval from  $-90$  to  $-70$  mV, because the current/voltage relationship was almost linear for this interval. The slope conductance calculated for K30-Ringer as external solution was  $g_{\text{K30-Ringer}} = 4.6 \pm 4.1$  nS ( $n = 7$ , for hSK3) and  $4.4 \pm 4.6$  nS ( $n = 5$ , for hSK3\_ex4). Because the external solution contained only 30 mM K<sup>+</sup> ions, the conduc-

tance was smaller than that found for K-Ringer (containing 164.5 mM K<sup>+</sup>). After the application of 1 mM 1-EBIO, the slope conductance increased to  $25.1 \pm 17.0$  ( $n = 7$ , for SK3) and  $19.4 \pm 16.8$  nS ( $n = 5$ , for hSK3\_ex4). The concentration-response curves for both isoforms are shown in Fig. 8C. To estimate only the 1-EBIO-activated potassium current, the slope conductance found for K30-Ringer was subtracted from that observed after adding 1-EBIO to the external solution. The slope conductances were normalized for the slope conductance found for 1 mM 1-EBIO and plotted against the 1-EBIO concentration. Because it was not clear whether the activation of hSK3 isoforms reached their maximum in the presence of 1 mM 1-EBIO, the curves were fitted according to the equation  $g/g_{1 \text{ mM } 1\text{-EBIO}} = a_{\text{max}} - a_{\text{max}}/(1 + ([1\text{-EBIO}]/$

$EC_{50})^{n_H})$ , with  $a_{\text{max}}$  as maximum relative conductance and  $n_H$  as the Hill coefficient. Best fits for curves of both isoforms were achieved when the Hill coefficient was assumed to be  $n_H = 1.8$  and  $a_{\text{max}}$  of 1.03 and 1.04 for hSK3 and hSK3\_ex4, respectively. However, 1-EBIO showed a similar effect on both isoforms. The half-maximal activation concentrations ( $EC_{50}$ ) were calculated to be 0.17 mM (for hSK3) and 0.19 mM (for hSK3\_ex4). 1-EBIO has already been shown to be an activator of SK/IK channels with an  $EC_{50}$  ranging from 74  $\mu\text{M}$  for SK4/IK1 (Jensen et al., 1998) to 650  $\mu\text{M}$  for SK1 and SK2 (Pedarzani et al., 2001). The determined  $EC_{50}$  values for both hSK3 isoforms fits the previously published one for SK3 channels with an  $EC_{50} = 100 \mu\text{M}$  (Grunnet et al., 2001b). Therefore, the sensitivity of hSK3 channels to

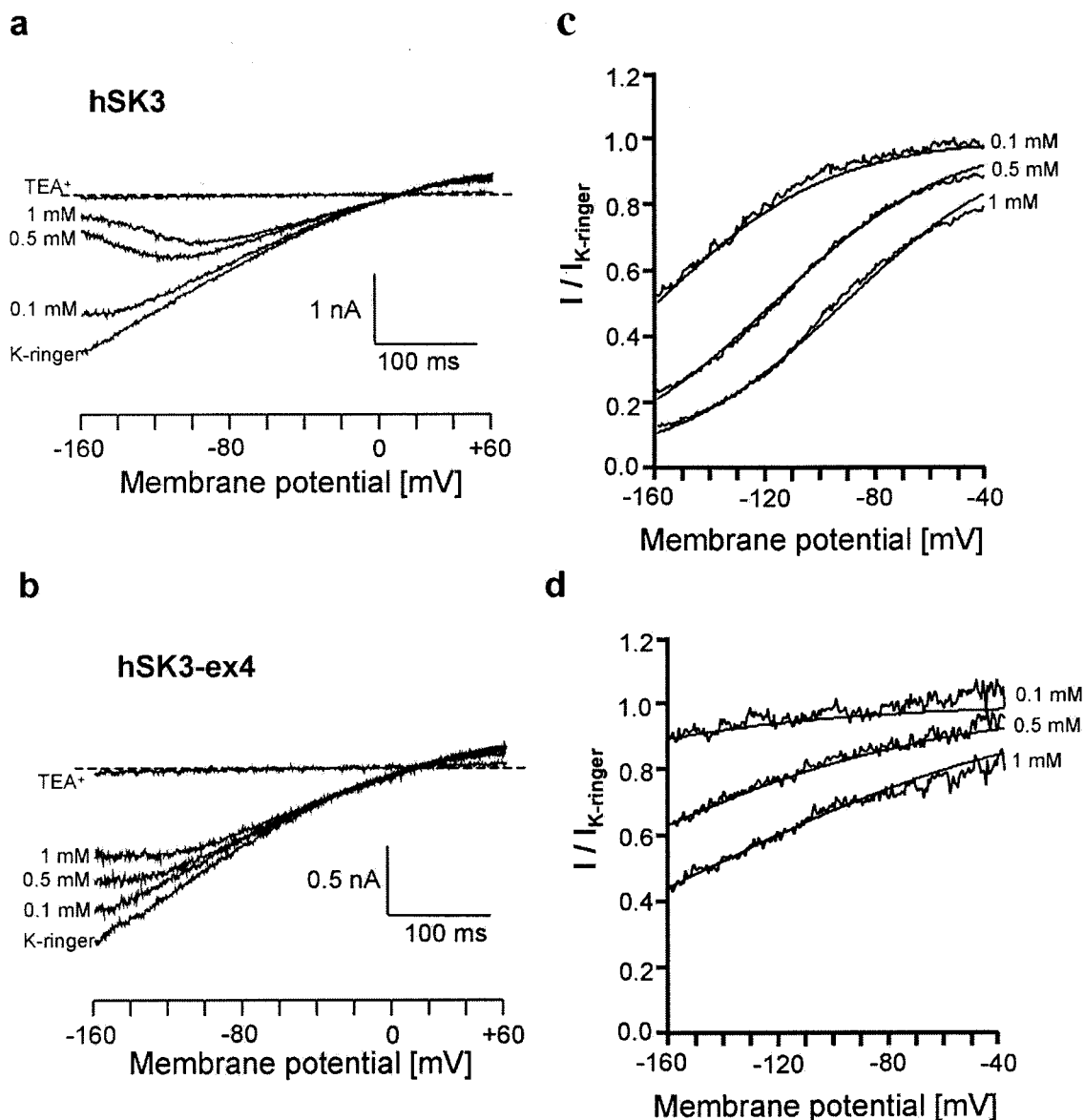


**Fig. 6.** External Ba<sup>2+</sup> block of currents through hSK3 and hSK3\_ex4. A and B, whole-cell currents for both isoforms. Currents were elicited by clamping the membrane potential in 400-ms ramps from -160 to +60 mV in TEA-Ringer (designated "TEA<sup>+</sup>" on the left) and K-Ringer with and without Ba<sup>2+</sup> (concentrations are given at the left of each trace). C and D, the voltage-dependence of the Ba<sup>2+</sup> block for hSK3 and hSK3\_ex4, respectively. Currents measured in TEA-Ringer were assumed as leak currents and were therefore subtracted from currents measured in K-Ringer with and without Ba<sup>2+</sup>. Relative currents were calculated as fractions of currents with K-Ringer as external solution. The mean relative currents were plotted as the mean of three experiments against the membrane potential for the interval from -160 to -40 mV. Smooth curves represent best fits of the Boltzmann equation  $I/I_{\text{K-Ringer}} = 1/(1 + \exp((E_{0.5} - E)/k))$ , with a steepness factor of  $k = 32$  mV for hSK3 (C) and  $k = 61$  mV for hSK3\_ex4 (D).  $E_{0.5}$  values calculated for both isoforms are given in the text.

1-EBIO is more similar to SK4/IK1 channels than to other SK channels.

**Activation of hSK3 and hSK3\_ex4 by Intracellular  $\text{Ca}^{2+}$ .** The experimental procedure allowed the measurement of whole-cell conductance and the internal  $\text{Ca}^{2+}$  concentration in parallel (Fig. 9). After subtracting the intensity of the autofluorescent light and calculating the ratio for F1 and F2 of the fura measurements as described above, the  $\text{Ca}^{2+}$  concentrations were calculated according to the equation  $[\text{Ca}^{2+}] = 1.63 \times (R - 0.21)/(2.2 - R)$ . The initial internal  $\text{Ca}^{2+}$  concentrations immediately after perfusion of the cell with the pipette solution varied between the cells and were found to be  $>1.6 \mu\text{M}$ . Within 5 to 10 min, the  $\text{Ca}^{2+}$  concentration decreased and reached concentrations ranging between 0.3 and  $0.12 \mu\text{M}$  (Fig. 9, A and B). Saturated maximum whole-cell conductances were observed for  $\text{Ca}^{2+}$  concentrations larger than  $1.5 \mu\text{M}$  and varied from 3.0 to 11 nS. The mini-

mum conductance was achieved for  $\text{Ca}^{2+}$  concentrations lower than  $0.3 \mu\text{M}$ , it ranged between 2.5 and 0.1 nS, and it was not subtracted as background conductance. The whole-cell conductance was plotted against  $\text{Ca}^{2+}$  concentrations for each experiment separately, and curves were fitted according to the equation  $g = g_{\text{max}} - a_1/(1 + ([\text{Ca}^{2+}]/\text{EC}_{50})^{n_H})$ , where  $g_{\text{max}}$  is the maximal conductance,  $\text{EC}_{50}$  is the half-maximal activating  $\text{Ca}^{2+}$  concentration, and  $n_H$  is the Hill coefficient (Fig. 9, E and F). Because the minimal conductance was not subtracted,  $a_1$  was assumed not to be equal to  $g_{\text{max}}$ . The  $\text{EC}_{50}$  and  $n_H$  values were calculated for each isoform as mean values ( $n = 3$ ) and were found to be  $0.91 \pm 0.4 \mu\text{M}$  and  $3.3 \pm 0.5$  for hSK3 and  $0.78 \pm 0.2 \mu\text{M}$  and  $4.1 \pm 0.2$  for hSK3\_ex4, respectively. The difference between the  $\text{EC}_{50}$  values was found to be not significant by applying a two-tailed Student's  $t$  test ( $p = 0.63$ ).

## Discussion

Alternative splicing is a common feature of mammalian potassium channel transcripts. It leads to altered functional properties of potassium currents by generating different isoforms. Therefore, it plays a vital role in the fine-tuning of whole-cell currents and the adjustment of potassium currents to the requirements of a particular cell (Coetzee et al., 1999). Sixteen isoforms, all generated by alternative splicing, were recently described for the SK1 channel in mouse (Shmukler et al., 2001). A similar pattern of alternative splicing was also described for transcripts of the human SK1/KCNN1 gene (Zhang et al., 2001). Because the splicing in those cases predominantly affected the calmodulin binding site, it was believed that the activation of SK1 channels can be modulated by altering their ability to bind calmodulin. The hSK3 isoforms described here were generated by the alternative inclusion of the discovered new exon 4. They differ in their amino acid sequence by an insertion of 15 amino acids into the extracytosolic region between the fifth transmembrane helix and the P-loop region of SK3. We were intrigued that perhaps this novel isoform might refine our understanding of the pharmacological as well as physiological properties of the channel. To test whether the pore region of SK3 channels is affected by the 15 amino acid insertion, we tested different blockers that are known to bind at the outer vestibule, such as TEA<sup>+</sup> (Bretschneider et al., 1999), *d*-tubocurarine, apamin (Ishii et al., 1997), and ScTX (Shakkottai et al., 2001). The S5–P-loop–S6 regions of SK2 and SK3 channels differ only at the residues Val485 and His521, which correspond to Val47 and Val95 in the KcsA channel and Tyr415 and Val451 in the *Shaker* potassium channel. The corresponding residues for SK2 are Ala331 and Asn367. This amino acid variation could be the reason for the different sensitivities of SK2 and SK3 channels to ScTX and might be essential for ScTX binding. Mutant cycle studies indicated that Val485 and His521 are near each other (Shakkottai et

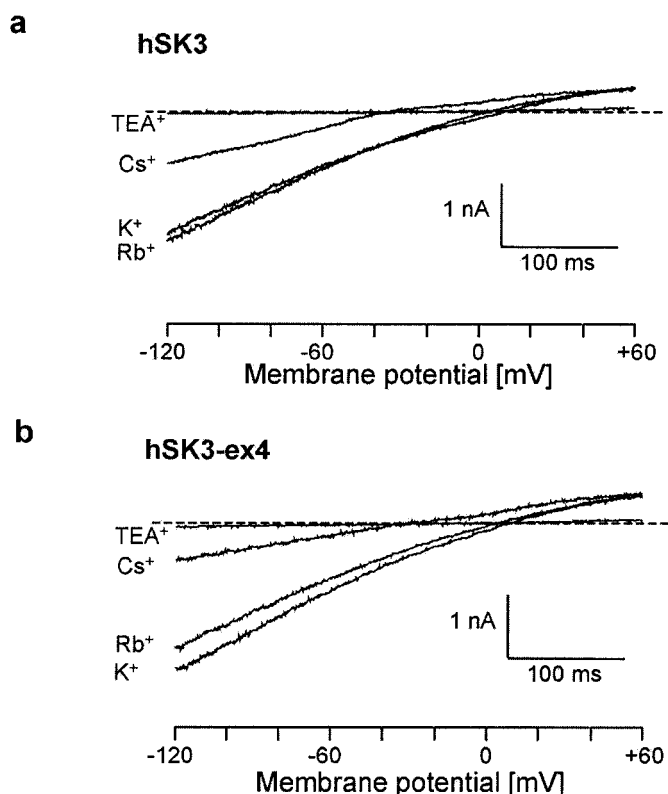


**Fig. 7.** Selectivity of hSK3 and hSK3\_ex4 to Cs<sup>+</sup> and Rb<sup>+</sup>. A and B, whole-cell currents, which were elicited by clamping the membrane potential in 400-ms ramps from  $-120$  to  $+60$  mV in TEA-Ringer, K-Ringer, Cs-Ringer, Rb-Ringer, and K0-Ringer solutions. Currents measured in TEA-Ringer were considered leak currents and therefore were subtracted from currents measured in other solutions. The whole-cell conductances were calculated from the slope of whole-cell currents for the interval ranging from  $-90$  to  $-70$  mV after leak currents were subtracted. The reversal potentials ( $E_{\text{rev}}$ ) were also determined after leak currents were subtracted. Relative conductances and permeabilities were calculated as fractions of whole-cell conductances and permeabilities observed in K-Ringer as external solution. Values are given in Table 1.

TABLE 1

Selectivity of hSK3 and hSK3\_ex4 to Rb<sup>+</sup> and Cs<sup>+</sup>. The mean values of three experiments are provided. Errors are given as S.D.

	$\Delta E = E_{\text{rev}} - E_{\text{rev(K-Ringer)}}$		P/P <sub>K-Ringer</sub>		g/g <sub>K-Ringer</sub>	
	hSK3	hSK3_ex4	hSK3	hSK3_ex4	hSK3	hSK3_ex4
Rb-Ringer	$-6 \pm 1.2\text{mV}$	$-5 \pm 2.4\text{mV}$	$0.79 \pm 0.04$	$0.8 \pm 0.07$	$1.1 \pm 0.15$	$0.77 \pm 0.14$
Cs-Ringer	$-45 \pm 6.0\text{mV}$	$-46 \pm 7.7\text{mV}$	$0.17 \pm 0.04$	$0.17 \pm 0.05$	$0.55 \pm 0.29$	$0.21 \pm 0.10$

al., 2001). The insertion of the additional amino acids in hSK3\_ex4 occurs only three amino acids C-terminal from Val485, and it is possible that they separate Val485 and His521 from each other in hSK3\_ex4. Such a conformational alteration of the outer vestibule in hSK3\_ex4 might well explain the strongly reduced ScTX sensitivity of this isoform as well as its reduced sensitivity to *d*-tubocurarine and apamin. Interestingly, the TEA<sup>+</sup> block was identical for both isoforms. For Kv1.1 channels, it has been shown that the TEA<sup>+</sup> binding is close to the selectivity filter within the P-loop region (Yellen et al., 1991; Bretschneider et al., 1999). Because this region is not interrupted by the inserted amino

acids in hSK3\_ex4, the TEA<sup>+</sup> binding sites of hSK3\_ex4 would be assumed not to be affected by the insertion. Therefore, we conclude that the inner regions of the vestibule remain unaffected by the additional amino acids of hSK3\_ex4. This is also reflected by the similar permeabilities of both isoforms to Cs<sup>+</sup> and Rb<sup>+</sup> ions. Surprisingly, the Ba<sup>2+</sup> block differs between hSK3 and hSK3\_ex4. The voltage-dependence of the Ba<sup>2+</sup> block observed for hSK3 in this report as well as that observed for the Ba<sup>2+</sup> block of other SK/IK channels (Hanselmann and Grissmer, 1996) indicates that the Ba<sup>2+</sup> binding site lies roughly halfway through the electrical field of the plasma membrane. The fact that the steep-

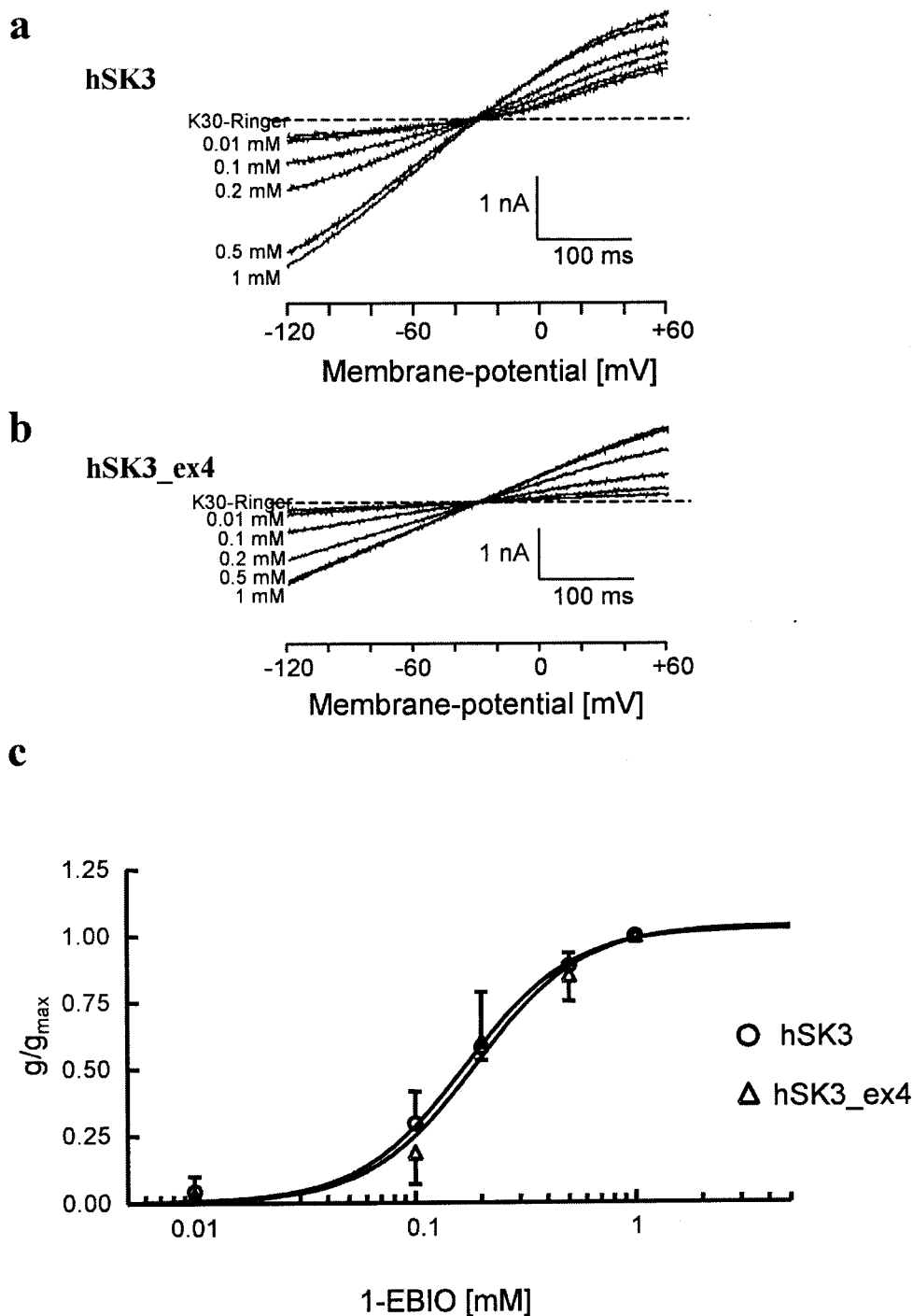


**Fig. 8.** Activation of currents through hSK3 and hSK3\_ex4 by 1-EBIO. A and B, whole-cell currents of hSK3 and hSK3\_ex4. Currents were elicited by 400-ms ramps from  $-120$  to  $+60$  mV in K30-Ringer with and without 1-EBIO (concentrations are given at the left of each trace). C, concentration-response curves of both isoforms for 1-EBIO. Whole-cell conductances were calculated from the slope of the ramp currents for the interval from  $-90$  to  $-70$  mV. The conductance found for currents in K30-Ringer were subtracted from conductances in K30-Ringer with 1-EBIO. Relative conductances were calculated as fractions of conductance in K30-Ringer with 1 mM 1-EBIO and were plotted against 1-EBIO concentrations. Curves were fitted according to  $g/g_{1 \text{ mM } 1\text{-EBIO}} = a_{\text{max}} - a_{\text{max}} / (1 + ([1\text{-EBIO}] / EC_{50})^{n_H})$ , where  $a_{\text{max}}$  is the maximal relative conductance calculated to be 1.03 for hSK3 and 1.04 for hSK3\_ex4. The Hill coefficient was calculated to be  $n_H = 1.8$  for both isoforms. For hSK3, the  $EC_{50}$  was calculated to be 0.17 mM and for hSK3\_ex4 to be 0.19 mM.

ness of voltage dependence of the  $Ba^{2+}$  block is reduced for hSK3\_ex4 indicates that the  $Ba^{2+}$  binding site is shifted toward the outside of the electrical field. It is still not clear whether the additional 15 amino acids in hSK3\_ex4 create a new  $Ba^{2+}$  binding site at a more exterior position of the vestibule or whether they change the properties of the electrical field at the outer vestibule of hSK3\_ex4.

The  $EC_{50}$  values for  $Ca^{2+}$  activation found for both isoforms showed no significant differences, indicating that the insertion of the 15 amino acids did not interfere with the activation of hSK3 channels by  $Ca^{2+}$ . Interestingly, the values found for hSK3 were higher than the ones described in previous reports, in which an  $EC_{50}$  ranging from 0.1 to 0.3  $\mu M$  was described previously (Köhler et al., 1996; Carignani et al., 2002). However, we were able to potentiate SK3 currents through both isoforms with 1-EBIO after whole-cell perfusion with 1  $\mu M$  free  $Ca^{2+}$ . Because 1-EBIO activates SK currents only in the pres-

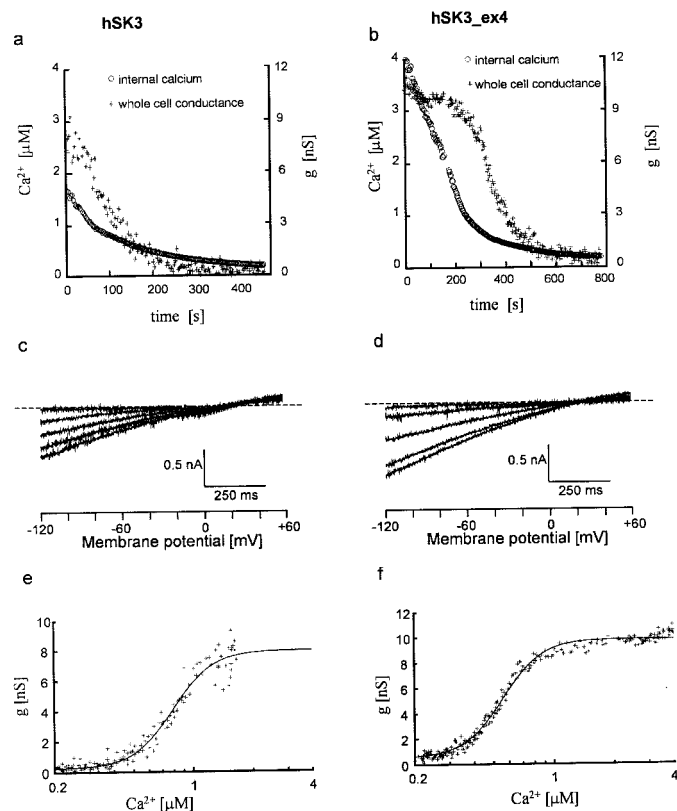


**Fig. 9.** Activation of hSK3 and hSK3\_ex4 by internal  $Ca^{2+}$ . Membrane potentials were clamped from  $-120$  to  $+60$  mV in 1-s ramps. The internal  $Ca^{2+}$  concentrations were measured in parallel using the fura-2 method. K-Ringer was used as external solution. Pipettes were filled with 2 to 4  $\mu l$  of tip solution containing 2  $\mu M$  free  $Ca^{2+}$  and 1 mM EGTA, which was overlaid with pipette-solution containing 10 mM EGTA without any  $Ca^{2+}$ . Whole-cell conductances were calculated for the interval from  $-90$  to  $-70$  mV. Internal  $Ca^{2+}$  concentration and whole-cell conductance are plotted against time (shown in A for hSK3 and in B for hSK3\_ex4). In both cases a continuous decrease of the internal  $Ca^{2+}$  concentration is paralleled by a decrease of whole-cell conductance. C and D, representative current ramps are given for both isoforms. For calculating the  $EC_{50}$  for  $Ca^{2+}$  of hSK3 and hSK3\_ex4, whole-cell conductances were plotted against the internal  $Ca^{2+}$  concentration for each experiment separately. Curves were fitted according to the equation  $g = g_{max} - a_1 / (1 + ([Ca^{2+}] / EC_{50})^{n_H})$ , where  $g_{max}$  is the maximal conductance and  $n_H$  is the Hill coefficient. Because the minimal conductance was not subtracted,  $a_1 \neq g_{max}$ . The Hill coefficient and the  $EC_{50}$  were calculated for each isoform as means of three independent experiments and were found to be  $0.91 \pm 0.4$   $\mu M$  and  $3.3 \pm 0.5$  for hSK3 and  $0.78 \pm 0.2$   $\mu M$  and  $4.1 \pm 0.2$  for hSK3\_ex4, respectively.

ence of  $Ca^{2+}$  at concentrations lower than those necessary for maximal activation (Pedarzani et al., 2001), this indicates that the 1  $\mu M$  free  $Ca^{2+}$  used in our experiments does not lead to a maximum activation of whole-cell SK3 currents. Therefore, this result is in line with the unexpectedly high  $EC_{50}$  values found for hSK3 and hSK3\_ex4.

SK channels underlie the AHP in excitable cells (Köhler et al., 1996; Stocker et al., 1999; Sah and Faber, 2002). The AHP in the rat CA1 hippocampal pyramidal neurons can be subdivided into scyllatoxin- and apamin-sensitive and -insensitive components (Stocker et al., 1999). The channels that underlie the scyllatoxin- and apamin-insensitive components of the AHP are also recognized to be insensitive to *d*-tubocurarine; however, their molecular nature remains unknown. Here, we describe an SK3 isoform that is insensitive to apamin, ScTX, and *d*-tubocurarine. If human excitable cells show a scyllatoxin- and apamin-sensitive component of the AHP, like CA1 pyramidal cells in rat, then the hSK3\_ex4 isoform might also generate a scyllatoxin- and apamin-insensitive component of the AHP similar to that observed in rat and guinea pigs. The molecular mechanism for the apamin- and ScTX-insensitive AHP component in humans, rats, and guinea pigs, however, seems to be different, mainly for two reasons. First, in rat (Stocker et al., 1999) and in guinea pigs (Martinez-Pinna et al., 2000; Vogalis et al., 2002), the apamin-insensitive component of the AHP was shown to be also TEA<sup>+</sup>-insensitive up to 10 mM. Second, a blast search did not reveal an orthologous exon 4 in rat. However, isoforms of SK channels, such like isoform hSK3\_ex4, may be good candidates for contributing to the molecular basis of the apamin-insensitive AHP component.

The TaqMan RT-PCR was used to quantify transcripts for both isoforms in different tissues. These experiments showed that both isoforms are coexpressed in most of the examined tissues, but that the hSK3\_ex4 transcript is expressed at much lower levels than hSK3 transcripts. The low amount of hSK3\_ex4 transcript would suggest a minor role for hSK3\_ex4 in vivo. However, the low expression level of hSK3\_ex4 transcripts might reflect the fact that hSK3\_ex4 is only expressed at higher levels in particular cells of a heterogeneous cell population. Furthermore, the possibility of heteromultimerization with other SK channel subunits might increase the number of SK channels per cell with pharmacokinetic properties similar to those of the hSK3\_ex4 isoform.

The fact that hSK3\_ex4 exhibits different pharmacological properties compared with hSK3 adds additional molecular support for current views of the site of action of these drugs and raises the possibility that SK3 currents through each isoform might be selectively modulated by specific drugs. This aspect may have heightened importance in view of the fact that the isoform hSK3 has been demonstrated to be a target for antipsychotic drugs (Terstappen et al., 2001).

#### Acknowledgments

We are grateful to Drs. Martin Hug, Jens Leipziger, Heike Jäger, and Gerd Scherer for helpful discussion and to Professor Ulrich Wolf for support.

#### References

- Bretschneider F, Wrisch A, Lehmann-Horn F, and Grissmer S (1999) External tetraethylammonium as a molecular caliper for sensing the shape of the outer vestibule of potassium channels. *Biophys J* 76:2351-2360.
- Carignani C, Roncarati R, Rimini R, and Terstappen GC (2002) Pharmacological and

- molecular characterisation of SK3 channels in the TE671 human medulloblastoma cell line. *Brain Res* **939**:11–18.
- Chandy KG, Fantino E, Wittekindt O, Kalman K, Tong LL, Ho TH, Gutman GA, Crocq MA, Ganguli R, Nimgaonkar V, et al. (1998) Isolation of a novel potassium channel gene HSKCa3 containing a polymorphic CAG repeat: a candidate for schizophrenia and bipolar disorder? *Mol Psychiatry* **3**:32–37.
- Chicchi GG, Gimenez-Gallego G, Ber E, Garcia ML, Winquist R, and Cascieri MA (1988) Purification and characterization of a unique, potent inhibitor of apamin binding from *Leiurus quinquestriatus hebraeus* venom. *J Biol Chem* **263**:10192–10197.
- Church GM and Gilbert W (1985) The genomic sequencing technique. *Prog Clin Biol Res* **177**:17–21.
- Coetzee WA, Amarillo Y, Chiu J, Chow A, Lau D, McCormack T, Moreno H, Nadal MS, Ozaita A, Pountney D, et al. (1999) Molecular diversity of K<sup>+</sup> channels. *Ann NY Acad Sci* **868**:233–285.
- Fanger CM, Ghanshani S, Logsdon NJ, Rauer H, Kalman K, Zhou J, Beckingham K, Chandy KG, Cahalan MD, and Aiyar J (1999) Calmodulin mediates calcium-dependent activation of the intermediate conductance KCa channel, IKCa1. *J Biol Chem* **274**:5746–5754.
- Fohr KJ, Warchol W, and Gratzl M (1993) Calculation and control of free divalent cations in solutions used for membrane fusion studies. *Methods Enzymol* **221**:149–157.
- Grunnet M, Jensen BS, Olesen SP, and Klaerke DA (2001a) Apamin interacts with all subtypes of cloned small-conductance Ca<sup>2+</sup>-activated K<sup>+</sup> channels. *Pflug Arch Eur J Physiol* **441**:544–550.
- Grunnet M, Jespersen T, Angelo K, Frokjaer-Jensen C, Klaerke DA, Olesen S, and Jensen BS (2001b) Pharmacological modulation of SK3 channels. *Neuropharmacology* **40**:879–887.
- Hamill OP, Marty A, Neher E, Sakmann B, and Sigworth FJ (1981) Improved patch-clamp techniques for high-resolution current recording from cells and cell-free membrane patches. *Pflug Arch Eur J Physiol* **391**:85–100.
- Hanselmann C and Grissmer S (1996) Characterization of apamin-sensitive Ca<sup>2+</sup>-activated potassium channels in human leukaemic T lymphocytes. *J Physiol* **496**:627–637.
- Hille B (2001) *Ion Channels of Excitable Membranes*, 3rd ed, Sinauer Associates INC, Sunderland, MA.
- Ishii TM, Maylie J, and Adelman JP (1997) Determinants of apamin and D-tubocurarine block in SK potassium channels. *J Biol Chem* **272**:23195–23200.
- Jensen BS, Strobaek D, Christophersen P, Jorgensen TD, Hansen C, Silahtaroglu A, Olesen SP, and Ahring PK (1998) Characterization of the cloned human intermediate-conductance Ca<sup>2+</sup>-activated K<sup>+</sup> channel. *Am J Physiol* **275**:C848–C856.
- Köhler M, Hirschberg B, Bond CT, Kinzie JM, Marrion NV, Maylie J, and Adelman JP (1996) Small-conductance, calcium-activated potassium channels from mammalian brain. *Science (Wash DC)* **273**:1709–1714.
- Martinez-Pinna J, Davies PJ, and McLachlan EM (2000) Diversity of channels involved in Ca<sup>2+</sup> activation of K<sup>+</sup> channels during the prolonged AHP in guinea-pig sympathetic neurons. *J Neurophysiol* **84**:1346–1354.
- Navaratnam DS, Bell TJ, Tu TD, Cohen EL, and Oberholtzer JC (1997) Differential distribution of Ca<sup>2+</sup>-activated K<sup>+</sup> channel splice variants among hair cells along the tonotopic axis of the chick cochlea. *Neuron* **19**:1077–1085.
- Nehls M and Boehm T (1995) A rapid and efficient alternative to sonication in shot-gun sequencing projects. *Trends Genet* **11**:39.
- Pedarzani P, Mosbacher J, Rivard A, Cingolani LA, Oliver D, Stocker M, Adelman JP, and Fakler B (2001) Control of electrical activity in central neurons by modulating the gating of small conductance Ca<sup>2+</sup>-activated K<sup>+</sup> channels. *J Biol Chem* **276**:9762–9769.
- Ramanathan K, Michael TH, Jiang GJ, Hiel H, and Fuchs PA (1999) A molecular mechanism for electrical tuning of cochlear hair cells. *Science (Wash DC)* **283**:215–217.
- Riley J, Butler R, Ogilvie D, Finniear R, Jenner D, Powell S, Anand R, Smith JC, and Markham AF (1990) A novel, rapid method for the isolation of terminal sequences from yeast artificial chromosome (YAC) clones. *Nucleic Acids Res* **18**:2887–2890.
- Rimini R, Rimland JM, and Terstappen GC (2000) Quantitative expression analysis of the small conductance calcium-activated potassium channels, SK1, SK2 and SK3, in human brain. *Brain Res Mol Brain Res* **85**:218–220.
- Rosenblatt KP, Sun ZP, Heller S, and Hudspeth AJ (1997) Distribution of Ca<sup>2+</sup>-activated K<sup>+</sup> channel isoforms along the tonotopic gradient of the chicken's cochlea. *Neuron* **19**:1061–1075.
- Sah P and Faber ES (2002) Channels underlying neuronal calcium-activated potassium currents. *Prog Neurobiol* **66**:345–353.
- Savic N, Pedarzani P, and Sciancalepore M (2001) Medium afterhyperpolarization and firing pattern modulation in interneurons of stratum radiatum in the CA3 hippocampal Region. *J Neurophysiol* **85**:1986–1997.
- Schumacher MA, Rivard AF, Bachinger HP, and Adelman JP (2001) Structure of the gating domain of a Ca<sup>2+</sup>-activated K<sup>+</sup> channel complexed with Ca<sup>2+</sup>/calmodulin. *Nature (Lond)* **410**:1120–1124.
- Shakkottai VG, Regaya I, Wulff H, Fajloun Z, Tomita H, Fathallah M, Cahalan MD, Gargus JJ, Sabatier JM, and Chandy KG (2001) Design and characterization of a highly selective peptide inhibitor of the small conductance calcium-activated K<sup>+</sup> channel, SkCa2. *J Biol Chem* **276**:43145–43151.
- Shmukler BE, Bond CT, Wilhelm S, Bruening-Wright A, Maylie J, Adelman JP, and Alper SL (2001) Structure and complex transcription pattern of the mouse SK1 K(Ca) channel gene, KCNN1. *Biochim Biophys Acta* **1518**:36–46.
- Stocker M, Krause M, and Pedarzani P (1999) An apamin-sensitive Ca<sup>2+</sup>-activated K<sup>+</sup> current in hippocampal pyramidal neurons. *Proc Natl Acad Sci USA* **96**:4662–4667.
- Strobaek D, Jorgensen TD, Christophersen P, Ahring PK, and Olesen SP (2000) Pharmacological characterization of small-conductance Ca<sup>2+</sup>-activated K<sup>+</sup> channels stably expressed in HEK 293 cells. *Br J Pharmacol* **129**:991–999.
- Sun G, Tomita H, Shakkottai VG, and Gargus JJ (2001) Genomic organization and promoter analysis of human KCNN3 gene. *J Hum Genet* **46**:463–470.
- Terstappen GC, Pula G, Carignani C, Chen MX, and Roncarati R (2001) Pharmacological characterisation of the human small conductance calcium-activated potassium channel hSK3 reveals sensitivity to tricyclic antidepressants and antipsychotic phenothiazines. *Neuropharmacology* **40**:772–783.
- Tomita H, Shakkottai VG, Gutman GA, Sun G, Bunney WE, Cahalan MD, Chandy KG, and Gargus JJ (2003) Novel truncated isoform of SK3 potassium channel is a potent dominant-negative regulator of SK currents: implications in schizophrenia. *Mol Psychiatry* **5**:524–535.
- Vogalis F, Harvey JR, and Furness JB (2002) TEA- and apamin-resistant K(Ca) channels in guinea-pig myenteric neurons: slow AHP channels. *J Physiol* **538**:421–433.
- Wolfart J, Neuheff H, Franz O, and Roeper J (2001) Differential expression of the small-conductance, calcium-activated potassium channel SK3 is critical for pacemaker control in dopaminergic midbrain neurons. *J Neurosci* **21**:3443–3456.
- Xia XM, Fakler B, Rivard A, Wayman G, Johnson-Pais T, Keen JE, Ishii T, Hirschberg B, Bond CT, Lutsenko S, et al. (1998) Mechanism of calcium gating in small-conductance calcium-activated potassium channels. *Nature (Lond)* **395**:503–507.
- Yellen G, Jurman ME, Abramson T, and MacKinnon R (1991) Mutations affecting internal tea blockades identify the probable pore-forming region of a K<sup>+</sup> channel. *Science (Wash DC)* **251**:939–942.
- Zhang BM, Kohli V, Adachi R, Lopez JA, Udden MM, and Sullivan R (2001) Calmodulin binding to the C-terminus of the small-conductance Ca<sup>2+</sup>-activated K<sup>+</sup> channel HSK1 is affected by alternative splicing. *Biochemistry* **40**:3189–3195.

**Address correspondence to:** Dr. Stephan Grissmer, Department of Applied Physiology, University of Ulm, Albert-Einstein-Allee 11, D-89081 Ulm, Germany. E-mail: stephan.grissmer@medizin.uni-ulm.de